WALAILAK JOURNAL
http://wjst.wu.ac.th Engineering and Physical Sciences

Modelling and Electrical Characteristics of the Thailand Plasma Focus-II (TPF-II)

Arlee TAMMAN[1], Mudtorlep NISOA[1,*], Boonchoat PAOSAWATYANYONG[2], Dheerawan BOONYAWAN[3], Nopporn POOLYARAT[4] and Thawatchai ONJUN[5]

[1]School of Science, Walailak University, Nakhon Si Thammarat 80161, Thailand
[2]Department of Physics, Faculty of Science, Chulalongkorn University, Bangkok 10330, Thailand
[3]Plasma and Beam Physics Research, Facility, Department of Physics and Materials Science, Faculty of Science, Chiang Mai University, Chiang Mai 50200, Thailand
[4]Faculty of Science and Technology, Thammasat University, Pathum Thani 12120, Thailand
[5]School of Manufacturing Systems and Mechanical, Engineering, Sirindhorn International Institute of Technology, Thammasat University, Pathum Thani 12120, Thailand

([*]Corresponding author's e-mail: nmudtorl@wu.ac.th)

Received: 17 April 2017, Revised: 23 June 2017, Accepted: 30 July 2017

Abstract

The Thailand Plasma Focus II (TPF-II) is a 3.3 kJ dense plasma focus that was developed at Walailak University, Thailand. The aim of the device is to study the production of ion beams in the keV energy range and their applications for the color modification of gemstones. A high-energy ion beam is produced by heating and acceleration in the pinch phase of the plasma focus. The heating process is determined by the maximum electrical current, which can be optimized by variation of the system's inductance. Lee model code was implemented to optimize the configuration of the electrodes. The current waveforms for the different initial conditions were used to obtain the system's inductance, which was verified by a short circuit test. It was found that the inductance and resistance were about 153 nH and 12 mΩ, respectively.

Keywords: Plasma focus, pinch phase, plasma sheath, short-circuit test, Lee model code

Introduction

Plasma focus (PF) devices are attractive for the production of dense energetic particles such as neutrons, ions, electrons, and photons. They can generate high temperatures and high-density plasmas in the order of the sun's plasma [1,2]. The PF device, shown in **Figure 1**, consists of a vacuum chamber, current collectors (anode and cathode collectors), a coaxial electrode, a high voltage capacitor, a high voltage power supply, a spark gap, and a trigger. The coaxial electrode consists of an inner electrode as the anode, an outer electrode as the cathode, and an insulator, as shown in **Figure 2**. The spark gap and current collector are connected to the power transmission unit, which is fabricated by the coaxial cables and crimp ring terminals. The anode and cathode are connected to the anode and cathode collectors, respectively. Thailand Plasma Focus-II (TPF-II) is a small plasma focus device, the second such plasma focus device designed and fabricated in Thailand [3]. The first one was the Thailand Plasma Focus-I (TPF-I), which was used to study Soft X-Ray (SXR) production [4]. The TPF-II is designed for the production of ion beams in the energy range of keV [5-7]. The device equivalent circuit is an RLC circuit [4,8-10]. The electrical parameters and the equivalent circuit of the plasma focus were used to compute a responding current consisting mainly of the frequency, maximum current, and damping parameter. The current is calculated by Eq. (1), which is composed of 3 parts: the current amplitude, exponential decrease, and oscillating term. The current waveform is shown in **Figure 3**. The angular frequency (ω) and the period (T) are calculated by Eqs. (2) and (3), respectively. The resistance (R) was neglected for Eqs. (2) and (3) because its value is very low.

$$I(t) = \frac{V_0}{\omega L} e^{-Rt/2L} \sin(\omega t) = I_0 e^{-Rt/2L} \sin(\omega t) \tag{1}$$

$$\omega = 1/\sqrt{L_0 C_0} \tag{2}$$

$$T = 2\pi\sqrt{L_0 C_0} \tag{3}$$

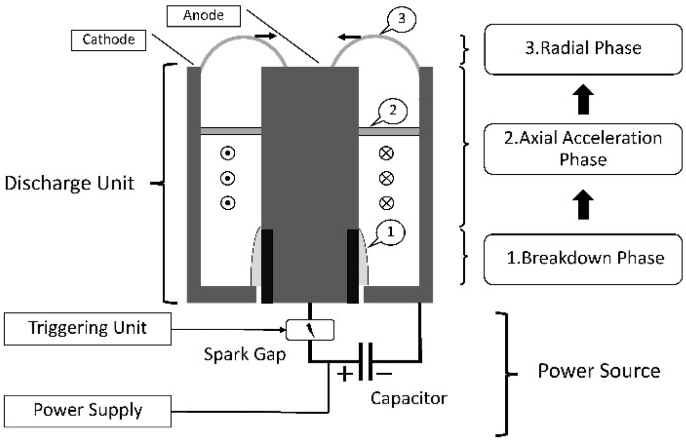

Figure 1 Plasma focus components and plasma discharge phases.

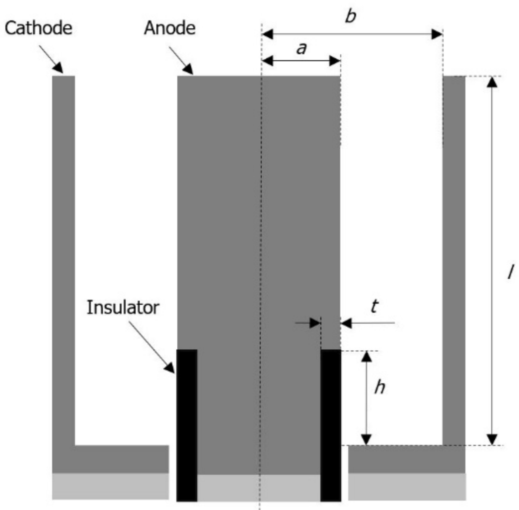

Figure 2 Cross section of electrode and insulator, anode radius (a), cathode radius (b), electrode length (l), effective insulator length (h), and insulator thickness (t).

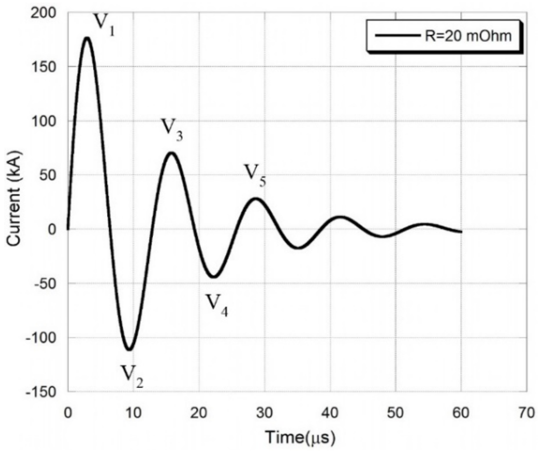

Figure 3 RLC current waveform with DPF parameter, R = 20 mΩ, C_0 = 30 μF, V_0 = 15 kV, and L_0 = 140 nH.

The inductance is very important for the operation of a plasma focus because it is the main component to determine T. The inductance can be separated into 2 parts, static inductance and varying inductance. The static inductance is the passive inductance of the component which consists of the capacitor, current collector, and spark gap. The varying inductance, which is adjusted by the number of coaxial cables, consists of the inductance of the coaxial cable and the inductance of the connector. The damping of the oscillating waveform in Eq. (1) is dependent on the inertial resistance (R_0) which is calculated by Eqs. (4) - (6) [8-11]. The voltage ratio of each maximum and minimum (f) is shown in **Figure 3**.

$$f_1 = \frac{V_2}{V_1}, f_2 = \frac{V_3}{V_2}, f_3 = \frac{V_4}{V_3}, f_4 = \frac{V_5}{V_4} \tag{4}$$

$$f = \frac{f_1 + f_2 + f_3 + f_4}{4} \tag{5}$$

$$R_0 = -\frac{2}{\pi} \ln|f| \sqrt{\frac{L_0}{C_0}} \tag{6}$$

The phenomenon of plasma focus begins with the gas breakdown between both electrodes near the insulator to generate a plasma sheath around the insulator, known as the breakdown phase. The movement of the plasma sheath along the electrode length, between the cathode and anode, from the lower side to the upper side, is the acceleration phase. The electrode length is optimized for the propagation of the plasma sheath to arrive at the top of anode with a maximum current. The propagation time of the plasma sheath is one fourth of the RLC oscillation period. At the top of the central electrode, the plasma pinch is induced by the collapse of the funnel-shape plasma sheath into the small volume, which is driven by the self-magnetic force ($J \times B$). The time when high temperature plasma particles are confined is called the pinch duration time.

The electrical parameters and efficiency of the plasma focus to produce ion beams depend on the configuration of the electrodes [12], gas pressure [13,14], and insulator [15,16]. In order to optimize the electrode structure, the anode radius (a), the ratio of the cathode and anode radii (c), the electrode length (l), and Lee model code [17-19] were used. The model consists of 3 groups of initial parameters: electrical parameters, gas parameters, and model parameters. By setting the initial parameters appropriately, the critical plasma focus parameters, pinch temperature, and pinch duration were calculated. Consequently, optimized values of *l, a*, and *c* were obtained.

Optimization of electrode components

TPF-II is a 3.3 kJ device with 30 μF of storage energy and 15 kV operating voltage. The structural configuration of the electrodes was obtained by calculation using the Lee model code. In the calculation, the initial parameters shown in **Table 1** were utilized. It was found that *c* and the effective electrode length (l_{eff}) were 2.0 and 11.5 cm, respectively. A quarter of the RLC periodic time is 3.04 μs, whereas the oscillating frequency, which was calculated by Eq. (2), is 82.19 kHz. The time variation of the current and voltage (IV curve) were obtained for a = 1.25 cm, b = 2.5 cm, and l_{eff} = 11.5 cm. It was found that the maximum current, the pinch duration, and the pinch temperature were 176 kA, 10.77 ns, and 421 eV, respectively.

Table 1 Initial parameters of plasma focus for calculation by Lee's Model.

Electrical Parameters	Gas Parameters	Model Parameters
C_0 = 30 μF	Gas Type: Neon	f_m = 0.1
L_0 = 125 nH	Pressure: 2.5 Torr	f_c = 0.7
R_0 = 2.3 mΩ		f_{mr} = 0.12
V_0 = 15 kV		f_{cr} = 0.68

Experimental setup

The short circuit test is the preliminary test of most PF devices and involves using a conductor plate (as shown in **Figure 4)** for connecting the cathode plate and anode. The short circuit test operated at 3 kV of capacitive charging voltage by varying the number of coaxial cables (2, 4, and 8), which were connected between the spark gap and current collector, as shown in **Figure 5**. The output waveform was used to calculate the inductance and resistance of the device. After the short circuit plate was connected, the electric charge was charged to the capacitor. When the spark gap was trigged by the triggering unit, the stored energy in the capacitor was transferred to the current collector. The current waveform was measured by the current probe.

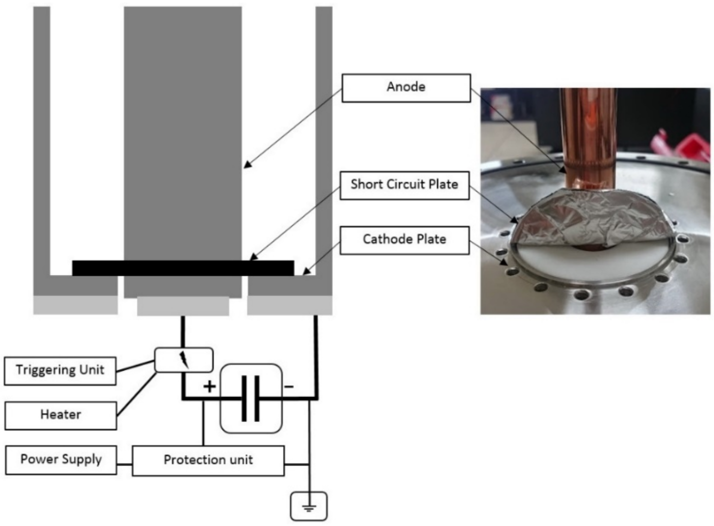

Figure 4 Diagram for short circuit test and pictures of anode, short circuit plate, and cathode plate.

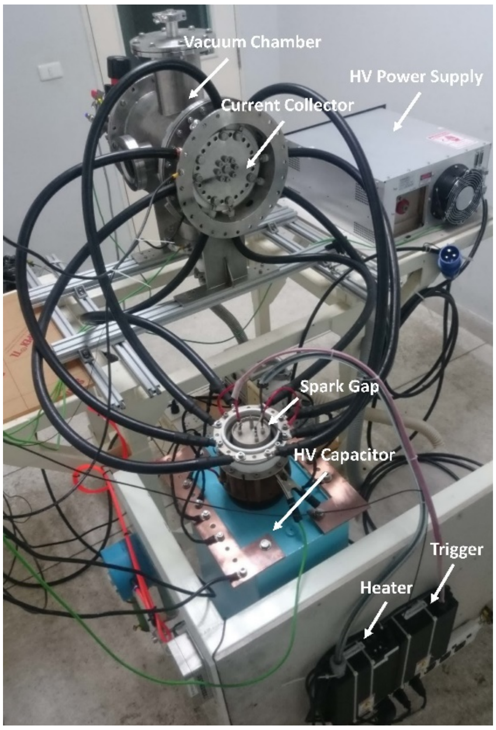

Figure 5 Picture of the connection between spark gap and current collector by 8 coaxial cables.

Results and discussion

An example of the current waveform, measured by the current probe, is shown in **Figures 6(a) - 6(c)** for 2, 4, and 8 coaxial cables, respectively. The inductance, calculated by Eq. (3) using T averaged over 3 periods and 5 repetitions, is shown in **Table 2**. The dependence of inductance on the number of coaxial cables from the calculations and experimental data are shown in **Figure 7**. There is some discrepancy between the calculated and experimental values and, thus, the experimental results were fitted by Eq. (7).

$$L_0 = 93 + 476 / n \tag{7}$$

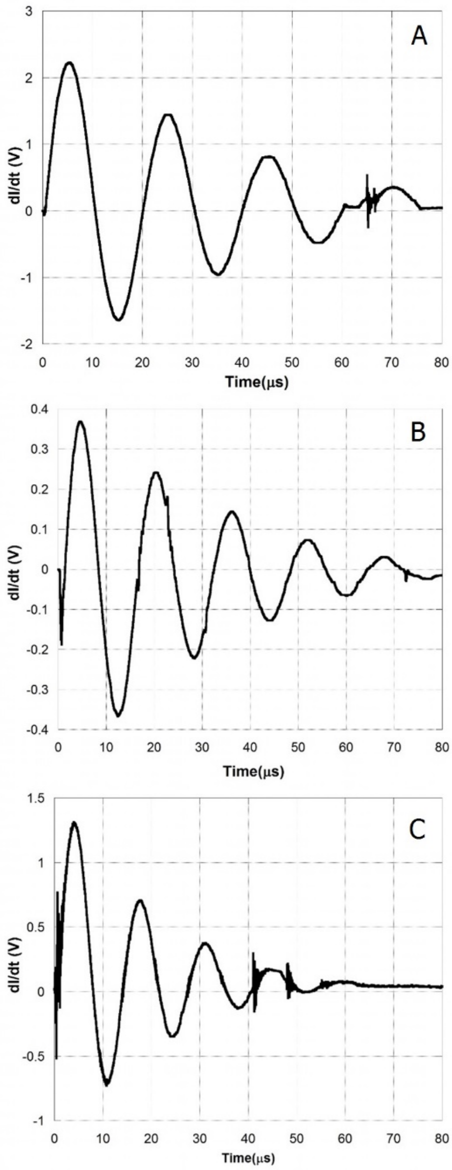

Figure 6 Signal of *dI/dt* of short circuit test for TPF-II using (a) 2, (b) 4, and (c) 8 lines of coaxial cable.

Table 2 Inertial inductance corresponding to number of coaxial cables of PF device, measured by short circuit test.

Number of Coaxial Cable	Inertial Inductance(nH)
2	334 ± 10
4	211 ± 5
8	153 ± 2

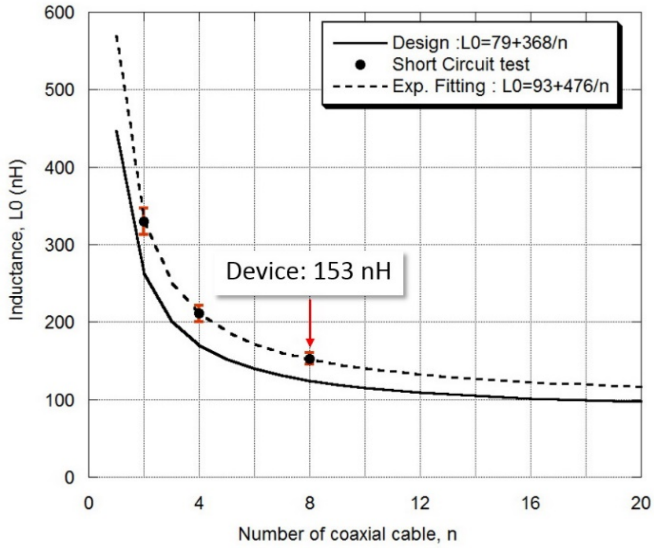

Figure 7 Inertial inductance of short circuit test and designed value.

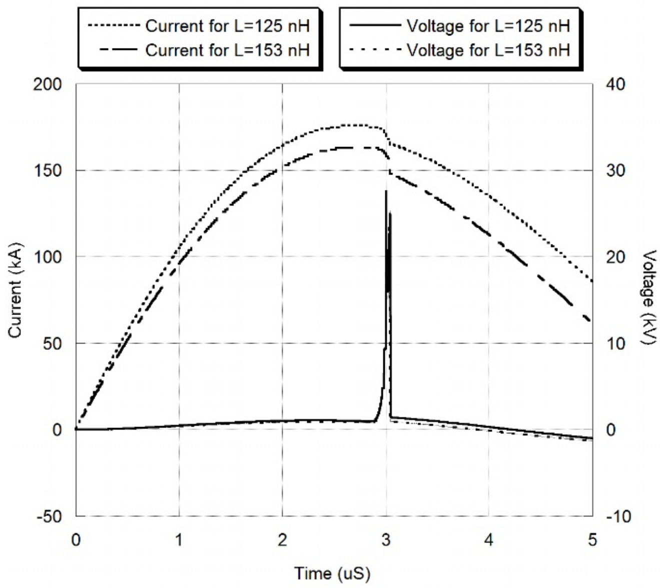

Figure 8 IV curve for system inductance L = 125 nH and 153 nH.

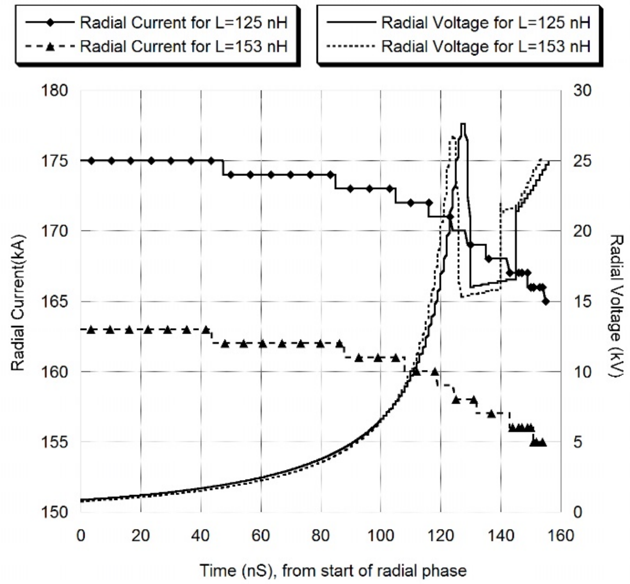

Figure 9 Radial phase IV curve for system inductance L = 125 nH and 153 nH.

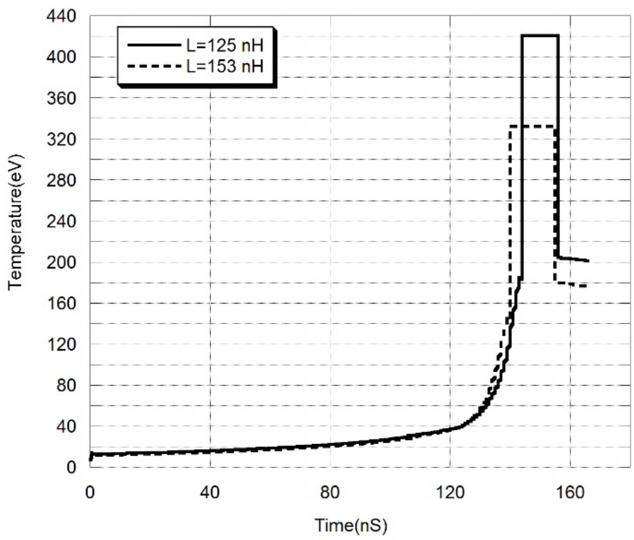

Figure 10 Time-dependent plasma temperature in radial phase for system inductance L = 125 nH and 153 nH.

The curve fitting shows that the experimental values of L_{static} and $L_{varying}$ were 93 and 476 nH, respectively. The slightly higher value of the static inductance was caused by fluctuations in the NX3 spark gap's inductance [20]. $L_{varying}$ increases due to 2 factors: 1) the connection between the coaxial cable and the spark gap, and 2) the connection between the coaxial cable and the current collector. The resistance of the system, which was calculated by Eq. (6), for 2, 4, and 8 coaxial lines, were 11 ± 1 mΩ, 10.1 ± 0.4 mΩ, and 12.0 ± 0.9 mΩ, respectively. From the short circuit test, the variation of the inertial inductance was 125 - 153 nH depending on the number of coaxial cables. The ultimate optimum electrode length, calculated by the Lee model code, was 11.2 cm. Therefore, the plasma focus parameters derived by the short circuit results for the IV curve, radial phase IV curve, and radial plasma temperature were acquired, and are shown in **Figures 8 - 10**, respectively. The maximum current and radial plasma temperature were lower than the initial calculated ones. The maximum current decreased from 176 kA to 163 kA. The pinch duration increased from 10.77 ns to 11.34 ns, whereas the pinch temperature decreased from 421 eV to 332 eV.

Conclusions

The preliminary result of the TPF-II short circuit test shows that the system inductance and resistance were 153 nH and 12 mΩ, respectively. The experimental results were used in the Lee model code to calculate the plasma focus's parameters. For neon gas discharge, we obtained an optimized length of 11.2 cm for the TPF-II's electrode, while a = 1.25 cm and b = 2.5 cm for 2.5 Torr of neon gas. The maximum current, pinch duration, and pinch temperature were found to be 163 kA, 11.34 ns, and 332 eV, respectively. The ion energy and flux measuring system will be installed in future work.

Acknowledgements

This work was supported by the Government Annual Research Budget through Thammasat University and Walailak University. The high-voltage power supply was provided by Chulalongkorn University and Chiang Mai University. A scholarship provided by the Human Resource Development in Science Project (Science Achievement Scholarship of Thailand, SAST). Finally, the authors would like to thank Prof. S. Lee for the model which is used in this research.

References

[1] L Soto. New trends and future perspectives on plasma focus research. *Plasma Phys. Contr. F* 2005; **47**, A361.

[2] A Bernard, H Bruzzone, P Choi, H Chuaqui, V Gribkov, J Herrera, K Hirano, A Krejei, S Lee, C Luo, F Mezzetti, M Sadowski, H Schmidt, K Ware, CS Wong and V Zoita. Scientific status of plasma focus research. *J. Moscow Phys. Soc.* 1998; **8**, 93-170.

[3] A Tamman, M Nisoa and T Onjun. Preliminary numerical study of Thailand Plasma Focus II (TPF-II) design. *Int. J. Mod. Phys. Conf. Ser.* 2014; **32**, 1460334.

[4] T Kunamaspakorn, N Poolyarat, R Picha, J Promping and T Onjun. Determination of the total inductance of TPF-I. *J. Phys. Conf. Ser.* 2015; **611**, 012009.

[5] J Jain, J Moreno, C Pavez, B Bora, M J Inestrosa-Izurieta, G Avaria and L Soto. Ion beam measurement using Rogowski coils in a hundred of joules dense plasma focus device. *J. Phys. Conf. Ser.* 2016; **720**, 12042.

[6] M Habibi. Angular distribution of ion beam emitted from a 3.5 kJ plasma focus device using different shapes of anodes. *Phys. Lett. A* 2016; **380**, 439-43.

[7] RA Behbahani and C Xiao. Common features of particle beams and x-rays generated in a low energy dense plasma focus device. *Phys. Plasmas* 2015; **22**, 1-6.

[8] AE Abdou, MI Ismail, AE Mohamed, S Lee, SH Saw and R Verma. Preliminary results of Kansas State University dense plasma focus. *IEEE Trans. Plasma Sci*. 2012; **40**, 2741-4.

[9] M Frignani, S Mannucci, D Mostacci, F Rocchi, M Sumini, E Angeli, A Tartari and L Karpinski. Short circuit tests on a 150 kJ, 1 Hz repetitive plasma focus. *Czech. J. Phys.* 2006; **56**, B413-B418.

[10] SH Saw and S Lee. Scaling laws for plasma focus machines from numerical experiments. *Energ. Power Eng.* 2010; **2**, 65-72.

[11] SH Saw, S Lee, F Roy, PL Chong, V Vengadeswaran, ASM Sidik, YW Leong and A Singh. *In situ* determination of the static inductance and resistance of a plasma focus capacitor bank. *Rev. Sci. Instrum*. 2010; **81**, 053505-9.

[12] N Talukdar, S Borthakur, NK Neog and TK Borthakur. Comparative study of neutron emission from a plasma focus device using two different anode shapes. *Phys. Plasmas* 2016; **23**, 52711.

[13] D Wong, A Patran, TL Tan, RS Rawat and P Lee. Soft X-ray optimization studies on a dense plasma focus device operated in neon and argon in repetitive mode. *IEEE Trans. Plasma Sci*. 2004; 32, 2227-35.

[14] H Bhuyan, H Chuaqui, M Favre, I Mitchell and E Wyndham. Ion beam emission in a low energy plasma focus device operating with methane. *J. Phys. D Appl. Phys*. 2005; **38**, 1164-9.

[15] HR Yousefi, FM Aghamir and K Masugata. Effect of the insulator length on Mather-type plasma focus devices. *Phys. Lett. A* 2007; **361**, 360-3.

[16] GR Etaati and M Ghorannevis. Insulator length effects in Mather: Type plasma focus device. *In*: Proceeding of the 31st EPS Conference on Plasma Physics. London, UK, 2004, p. 28-31.

[17] S Lee. An energy-consistent snow-plough model for pinch design. *J. Phys. D Appl. Phys*. 1983; **16**, 2463-74.

[18] S Lee and SH Saw. Numerical experiments providing new insights into plasma focus fusion devices. *Energies* 2010; **3**, 711-37.

[19] S Lee. Plasma focus radiative model: Review of the Lee Model Code. *J. Fusion Energ*. 2014; **33**, 319-35.

[20] R Verma, RS Rawat, P Lee, ATL Tan, H Shariff, GJ Ying, SV Springham, A Talebitaher, U Ilyas, and A Shyam. Neutron emission characteristics of NX-3 plasma focus device: Speed factor as the guiding rule for yield optimization. *IEEE Trans. Plasma Sci*. 2012; **40**, 3280-9.